



Shahid Chamran
University of Ahvaz

Journal of Applied and Computational Mechanics



Research Paper

Weighted Dual Approach to an Equivalent Stiffness-based Load Transfer Model for Jacked Open-ended Pile

Nguyen Ngoc Linh¹, Nguyen Anh Ngoc², Nguyen Van Kuu³, Nguyen Dang Diem⁴

¹ Department of Mechanical Engineering, Thuyloi University (TLU), Hanoi, Vietnam, Email: nnlinh@tlu.edu.vn

² Department of Mechanical Engineering, University of Transport and Communications (UTC), Hanoi, Vietnam, Email: nguyennanhngocmxm@utc.edu.vn

³ Department of Mechanical Engineering, Thuyloi University (TLU), Hanoi, Vietnam, Email: nguyenvankuu123@tlu.edu.vn

⁴ Department of Mechanical Engineering, University of Transport and Technology (UTT), Hanoi, Vietnam, Email: ndangdiem@gmail.com

Received May 14 2021; Revised June 18 2021; Accepted for publication June 22 2021

Corresponding author: N.N. Linh (nnlinh@tlu.edu.vn)

© 2021 Published by Shahid Chamran University of Ahvaz

Abstract. This paper presents a new equivalent stiffness-based load transfer model for an open-ended pipe pile. The main idea of this model is to replace the sum of unit stiffnesses corresponding with external and internal unit skin frictions in the basic differential equation of load transfer by a weighted average of equivalent unit stiffnesses using a dual approach of equivalent replacement. The contribution of external and internal skin frictions to equivalent unit stiffnesses is evaluated by normalized dimensionless weighting coefficients in the form of average value with the penetration depth. Application of new load transfer model to a jacked open-ended pile concerning semi-empirical models of external and internal unit skin frictions leads to corresponding explicit expressions of weighting coefficient. A computational example of a jacked open-ended pile is carried out. It is shown that the proposed equivalent stiffness-based load transfer model is an effective tool for analyzing behaviors of the open-ended pile in considering the soil plugging effect.

Keywords: Jacked open-ended pile; load transfer method; equivalent stiffness; dual approach of equivalent replacement.

1. Introduction

In recent years, open-ended pipe piles have played an increasingly important role in foundation engineering, from urban to coastal structures, due to their advantages of high bearing capacity, lightweight, and good performance. A particular feature of this pile that distinguishes it from others is the soil plugging effect which has attracted a lot of attention in research, design, and installation. The research trends mainly focus on the formation mechanism of the soil plug and the influence of the plugging effect on the open-ended pile driving as well as the bearing capacity of the pile, in both theoretical and experimental approaches.

Regarding experimental research, there have been many pioneering studies on these issues, thereby providing insight into the physical properties of open-ended piles. In [1], Paik and Lee organized a series of calibration chamber tests on open-ended pipe piles, they found that although the pile driven into sand remains partially plugged, the plug resistance is larger than or nearly equal to the outside shaft resistance in all cases of model tests. Paikowsky et al. [2] investigated the effect of soil plugging on the axial resistance developed by open-ended piles installed in sand and clay. The load carrying capacity of the internal soil plug has also been explored by Randolph et al. [3], [4] who showed that the capacity increases exponentially with plug length through one-dimensional analysis. And, authors proposed a distribution profile of lateral earth pressure coefficient along the length of the soil column. Interesting field observations of soil plug formation and soil arching are provided in [5]-[10], in semi-empirical methods to estimate the soil plug capacity and pile bearing capacity, including the incremental filling ratio *IFR*, and the plug length ratios *PLR*, where *PLR* is the ratio of the length of soil plug to pile penetration depth and *IFR* is the ratio of the increment of soil plug length to the increment of pile penetration depth. In application, different design methods for open-ended pipe piles are summarized in [11], [12] where a major factor for all design codes is to properly account for the formation and effects of soil plug.

Developing theoretical models to describe the behavior of open-ended piles in association with the plugging effect during driving, as well as to predict bearing capacity are issues of concern. The equilibrium of soil plug with the concept of active length developed by Randolph et al. [3], [4] based on the silo theory has become a basic theoretical model for reference with newly developed numerical studies. For example in [13], Henke and Grabe considered the influence of the installation methods on the soil plug behavior inside open-ended piles using software ABAQUS. In [14], Henke found that Coupled Eulerian-Lagrangian approach is a well-suited tool to investigate boundary value problems involving large deformations in the case of soil plugging inside tubular piles. Following this approach, several numerical simulations of the pile driving process in various soil conditions were implemented to investigate the effect of plugging with regard to different installation methods for jacked piles and dynamic driven piles in [15]-[17] based on Coupled Eulerian-Lagrangian and Discrete element methods. On the other hand, analytical approaches such as the load transfer method, although a widely used analytical tool in analyzing the responses of close-ended



piles, have not yet been able to be conveniently applied to open-ended piles. Due to the arching effect during pile driving, namely in unplugged and partially plugged states, parameters of the internal soil will be changed accordingly, from elastic model to rigid model [1]-[4], [18]. On the contrary, the behavior of open-ended piles is similar to that of closed-ended piles when the fully plugged state occurs, the internal skin friction is invalid [1], [2], this means in this state the responses of open-ended piles is the same as that of closed-ended piles. As a consequence, a major problem with the load transfer method is the difficulty in describing explicit expressions of the pile shaft stiffnesses related to plugged states in the basic differential equation of load transfer. It appears that the analysis of open-ended piles based on the load transfer models requires appropriate approaches. In [18], Liu et al. proposed a pile-in-pile model for studying the effect of the pile annulus and internal soil plug separately, i.e., the pile annulus as the “outer pile” and the soil plug as the “inner pile”, where different models were applied to external and internal skin frictions. The axial force and settlement of the open-ended pile shaft were computed by superposing the corresponding ones caused by the “outer pile” and the “inner pile”. However, this approach cannot provide a perspective about the reciprocal influence between external skin friction and its counterpart internal skin friction on the pile responses.

Recently, a dual approach has been proposed to investigate the response of nonlinear systems by Anh [19], and some dual techniques in equivalent replacement have been developed by Anh et al. [20]-[23]. Remarkably, in recent times a new weighted averaging criterion proposed in [23] derived from this approach has been successfully applied to wide classes of nonlinear problems by Hieu et al. [24]-[26]. The main issue of the dual approach to a replacing problem is to always consider two different (dual) aspects of the problem. This allows the analysis to become more harmonious and reflects the essence of the problem [22]. In this paper, we study a new load transfer model for a jacked open-ended pipe pile in considering the simultaneous influences of external and internal skin frictions on the displacement and axial force responses. For this purpose, a weighted dual equivalent replacement is used to describe the relationship between external and internal skin frictions with corresponding soil stiffnesses in the basic differential equation of load transfer.

The remainder of the paper is organized as follows. In Section 2, the basic differential equation of load transfer for an axially loaded open-ended pipe pile is considered first in concern with the load transfer for external and internal pile-soil interactions, as well as for the pile-soil interaction at the pile tip. Next, a weighted average of equivalent unit stiffnesses is introduced to replace the sum of unit stiffnesses in the basic differential equation of load transfer. The equivalent stiffness-based load transfer model is applied to a jacked open-ended pile in Section 3. Numerical examinations are carried out in Section 4. Section 5 contains the conclusions.

2. Equivalent stiffness-based load transfer model

2.1 Basic equation of load transfer

Axial displacement and axial force are two basic responses of an open-ended pipe pile under axial load which can be determined analytically by the load transfer method. In order to obtain these responses, we first consider the mechanism of pile-soil interaction for the open-ended pile. To simplify the analysis, it is assumed that the pile-soil interaction models are linear and the soil is homogenous, the body forces such as inertial and damping forces are neglected, which means that the superposition principle is valid.

Normally, the soil stiffnesses beneath the pile tip, around and inside the pile could be represented by the elastic properties of the spring. Hence, the pile-soil interaction can be analyzed through those elastic elements. As illustrated in Fig. 1.a, the pile-soil interaction at the pile tip is modeled by springs at the pile tip, while external and internal skin frictions at the pile shaft, $f_{s,e}$ and $f_{s,i}$, are modeled by springs with the corresponding unit stiffness coefficients k_e and k_i , respectively. $f_{s,e}$ is related to properties of external pile-soil interaction, meanwhile $f_{s,i}$ depends on the development of a soil plug forming inside the pile during driving. Adapting the linear dependence between the unit skin frictions and axial displacement of the pile $u_p(z)$, we then have the relationship:

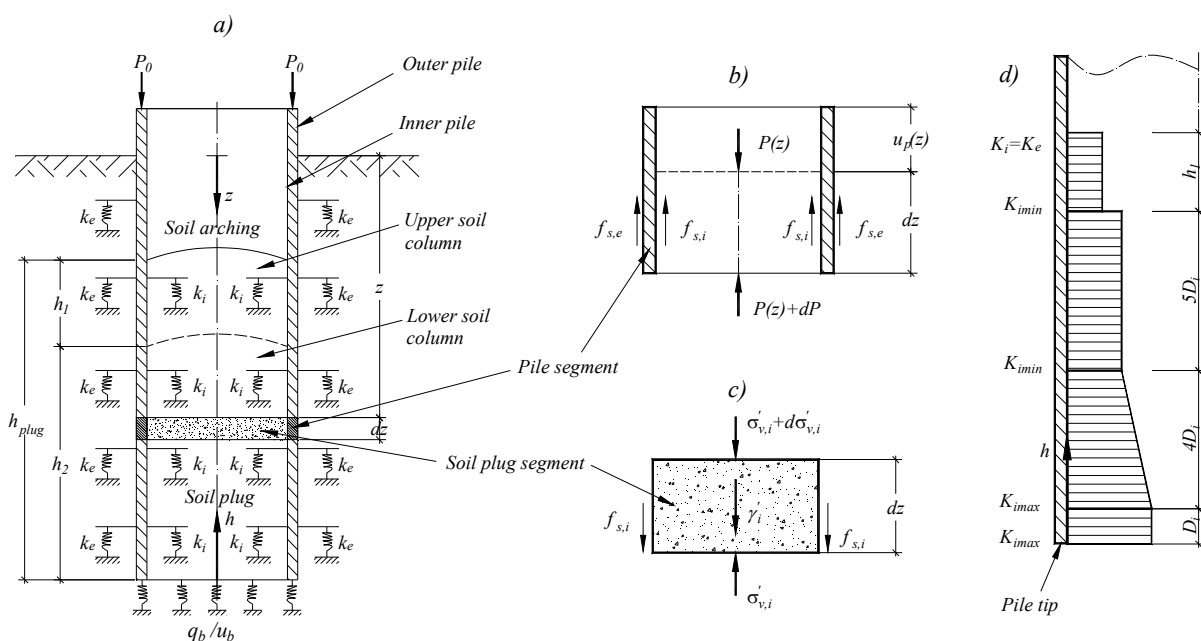


Fig. 1. a) Load transfer diagram of pile-soil interaction; b) Force equilibrium of a pile segment; c) Force equilibrium of a soil plug segment; d) Distribution of lateral earth pressure coefficient



$$f_{s,e}(z) = k_e u_p(z) \quad (1)$$

$$f_{s,i}(z) = k_i u_p(z) \quad (2)$$

Here the index “e”, “i” denote external and internal pile-soil interactions.

As shown in the literature, the open-ended pile is characterized by the plugging effect including three possible states in the driving process [1]-[5]:

- Unplugged state (I) involving the forming of the upper soil column with length h_1 during the initial pile driving. The effect of $f_{s,i}$ on the inner pile wall may be considered to be the same manner as that of $f_{s,e}$ but $f_{s,i}^{\text{II}} < f_{s,e}^{\text{II}}$;
- Partially plugged state (II) involving the forming of the lower soil column with length h_2 under the arching effect which restricts partially the external soil to enter inside the pile as $f_{s,i}^{\text{II}} \geq f_{s,e}^{\text{II}}$;
- Fully plugged state (III) occurs as the pile penetration continues but the soil plug length does not change due to the soil plug restricts fully external soil to enter the inside of the pile. Since then the pile acts as a close-ended one, the internal unit skin friction is invalid, $f_{s,i}^{\text{III}} = 0, k_i^{\text{III}} = 0$.

Clearly, k_e and k_i change with the variation of $f_{s,e}$ and $f_{s,i}$ during driving. It should be noted that for state III, the external unit skin friction of a close-ended pile can be derived from the elastic theory [27], [28]

$$f_{s,e}^{\text{III}}(z) = k_e^{\text{III}} u_p^{\text{III}}(z) \quad (3)$$

where

$$k_e^{\text{III}} = \frac{G_{s,e}}{r_e \zeta_e} \quad (4)$$

$$\zeta_e = \ln \left(\frac{r_{m,e}}{r_e} \right) \quad (5)$$

$$r_m = 2.5L(1 - \nu_s) \quad (6)$$

where $G_{s,e}$ and ν_s are respectively the shear modulus and Poisson's ratio of external soil, ζ_e is called the effective parameter of the outer pile radius r_e , L is the pile length. It is seen that Eq. (3) is a particular case of Eq. (1). For states I and II, the above expression of the external unit skin friction may be inapplicable due to the simultaneous interaction of external and internal skin frictions. For convenience, the formulations of $f_{s,e}, f_{s,i}, k_e$ and k_i for states I, II will be determined in the next sections.

Consider the force balance of an open-ended pile segment dz at a certain depth z as illustrated in Fig. 1.b. Given $f_{s,e}, f_{s,i}, k_e, k_i$ for three plugged states, the differential equation of the skin frictions to axial force $P(z)$ is defined by

$$\frac{dP(z)}{dz} = -2\pi(r_e f_{s,e} + r_i f_{s,i}) \quad (7)$$

where r_i is the pile inner radius. The development of axial force $P(z)$ due to axial displacement $u_p(z)$ is described by [27],[28]

$$P(z) = -E_p A_p \frac{du_p(z)}{dz} \quad (8)$$

where A_p is the pile section, E_p is the pile elastic modulus at the depth z . Using Eqs. (7) and (8), the basic differential equation of the load transfer method is governed by the following equation

$$\frac{d^2 u_p(z)}{dz^2} = \frac{2\pi(r_e f_{s,e} + r_i f_{s,i})}{E_p A_p} = \mu^2 u_p(z) \quad (9)$$

where noting the relationships (1),

$$\mu^2 = \frac{2\pi(r_e k_e + r_i k_i)}{E_p A_p} \quad (10)$$

The solution of Eq. (9) can be found in the form of

$$u_p(z) = C_1 e^{\mu z} + C_2 e^{-\mu z} \quad (11)$$

where C_1, C_2 are integral constants. According to load transfer for the pile tip, two boundary conditions supplemented to (9) are

$$\begin{aligned} \left. \frac{du_p(z)}{dz} \right|_{z=L} &= -\frac{Q_b(L)}{E_p A_p} \\ u_p(z) \Big|_{z=L} &= u_b \end{aligned} \quad (12)$$



where u_b and $Q_b(L)$ are soil settlement and ultimate bearing resistance at the full penetration depth $z = L$. In other words, the load-settlement relation of the pile base is used as limiting conditions for the pile at the full penetration depth, i.e. $u_p(z) \rightarrow u_b$, $P(z) \rightarrow Q_b(L)$ as $z \rightarrow L$. After determining C_1 and C_2 , the obtained displacement of a pile segment is

$$u_p(z) = \frac{u_b}{2} \left(1 - \frac{K_{ps}}{\mu} \right) e^{-\mu(L-z)} + \frac{u_b}{2} \left(1 + \frac{K_{ps}}{\mu} \right) e^{\mu(L-z)} \quad (13)$$

where

$$K_{ps} = \frac{Q_b(L)}{u_b E_p A_p} \quad (14)$$

Using displacement response (13) to solve Eq. (8), to give the expression of axial force $P(z)$

$$P(z) = \frac{Q_b(L)}{2} \left[\left(1 - \frac{\mu}{K_{ps}} \right) e^{-\mu(L-z)} + \left(1 + \frac{\mu}{K_{ps}} \right) e^{\mu(L-z)} \right] \quad (15)$$

The expressions of displacement and axial force responses of an open-ended pile given by Eqs. (13) and (15) show that the input parameters needed for analysis are the pile geometry, the elastic constants of soil and pile, and the soil stiffness coefficients. The physical interpretation of μ^2 in Eq. (10) and K_{ps} in Eq. (14) can be expressed as

$$\mu^2 = \frac{\text{total unit stiffness of pile shafts}}{\text{pile stiffness}}$$

$$K_{ps} = \frac{\text{unit stiffness of base soil}}{\text{pile stiffness}}$$

Remarkably, μ^2 and K_{ps} are the ratio of shaft-pile stiffness and the ratio of base-pile stiffness, respectively. The dimensions of μ and K_{ps} are both length^{-1} , thus the ratio of μ to K_{ps} is dimensionless. Clearly, the fully plugged state corresponding with $f_{s,i} = 0$, at this state $\mu^2 = 2\pi r_e k_e / E_p A_p$, and the basic equation of load transfer (9) reduces to the case of a close-ended pile with stiffness k_e^{III} , with the displacement and axial force responses as result shown in [28]. In the next section, the unknown unit stiffness coefficients of the pile shaft, $k_e^{I,II}$ and $k_i^{I,II}$, will be determined.

2.2 Equivalent unit stiffness coefficients in concern with the weighted dual approach

The fact is that the formulations of external and internal unit skin frictions for states I and II, $f_{s,e}^{I,II}$ and $f_{s,i}^{I,II}$, can be achieved from laboratory and in situ tests, normally to be considered as functions with the penetration depth or with the soil plug length [3], [18]. Nevertheless, it is necessary to determine formulations for corresponding stiffnesses, $k_e^{I,II}$ and $k_i^{I,II}$, to fully describe the load transfer model. An additional question then arises if there is a possible way to describe the influence of those unit skin frictions on these stiffnesses. The answers to the problems are shown below.

Physically, state III is a continuation of states I and II during the driving process. Therefore, it can be assumed that the pile shaft stiffnesses in states I and II are related to the ones in states III in homogenous soil. Adopting the dual approach in equivalent replacement [20]-[22], here we may use equivalent unit stiffness coefficients for $k_e^{I,II}, k_i^{I,II}$, that are derived from the available unit stiffness coefficient k_e^{III} given by Eq. (4). The equivalent replacements are illustrated schematically as follows

$$\begin{aligned} k_e^{I,II} &\rightarrow p_1 k_e^{\text{III}} \\ k_i^{I,II} &\rightarrow p_2 k_e^{\text{III}} \end{aligned} \quad (16)$$

where p_1, p_2 are weighting coefficients. In more general, applying (16) to Eq. (20), the sum of unit stiffnesses can be replaced by a weighted average

$$r_e k_e + r_i k_i \rightarrow p r_e k_e^{\text{III}} + (1-p) r_i k_e^{\text{III}} \quad (17)$$

where p is a normalized dimensionless weighting coefficient, satisfying the condition

$$0 < p \leq 1 \quad (18)$$

It is expected that the weighting coefficient p plays a role in adjusting the contributions of external skin friction $f_{s,e}^{I,II}$ and its counterpart internal skin friction $f_{s,i}^{I,II}$ in order to obtain the best replacement of $k_e^{I,II}$ and $k_i^{I,II}$ by k_e^{III} . In particular, the contributions of $f_{s,e}^{I,II}$ and $f_{s,i}^{I,II}$ to the total unit skin friction $f_{s,e}^{I,II} + f_{s,i}^{I,II}$ should be represented by p . Because $f_{s,e}^{I,II}$ and $f_{s,i}^{I,II}$ are functions that depend on z , while p is required to be non-dimensional, we therefore consider their realization in the mean sense, i.e. $\langle f_{s,e}^{I,II} \rangle$ and $\langle f_{s,i}^{I,II} \rangle$ versus $\langle f_{s,e}^{I,II} + f_{s,i}^{I,II} \rangle$, where the mean value $\langle \cdot \rangle$ is calculated by

$$\langle \cdot \rangle = \frac{1}{\Delta z} \int_{z_i}^{z_{i+1}} (\cdot) dz \quad (19)$$

with $\Delta z = z_{i+1} - z_i$ is the calculation interval of depth in which $f_{s,e}^{I,II}$ and $f_{s,i}^{I,II}$ vary. Accordingly, the weighting coefficients can be formulated by



$$p = \frac{\langle f_{s,e}^{I,II} \rangle}{\langle f_{s,e}^{I,II} + f_{s,i}^{I,II} \rangle}$$

$$1 - p = \frac{\langle f_{s,i}^{I,II} \rangle}{\langle f_{s,e}^{I,II} + f_{s,i}^{I,II} \rangle} \quad (20)$$

The above calculation procedure is called the equivalent stiffness-based load transfer model, from which the following remarks are made:

- The partially plugged state (II) starts happening as $f_{s,i}^{II} = f_{s,e}^{II}$, thus the corresponding value of the weighting coefficient for this boundary limit when transitioning from the unplugged state (I) to the partially plugged state (II) is $p = 1/2$.
- The fully plugged state (III) occurs as $f_{s,i} = 0$, it leads to $p = 1$. Hence $p = 1$ is related to the boundary limit when transitioning from the partially plugged state (II) to the fully plugged state (III).

3. Application of equivalent stiffness-based load transfer model to a jacked open-ended pile

In this section, the equivalent stiffness-based load transfer model is applied to a jacked open-ended pile in concern with the semi-empirical model of internal skin friction derived from tests by De Nicola and Randolph [3]. As the above assumption of linear pile-soil interaction, load transfer for an open-ended pile can be considered in three separate models, which are load transfer for the pile tip, load transfer for external and internal pile-soil interactions. To obtain explicit expressions of the weighting coefficient p , it is first necessary to determine formulations of external and internal unit skin frictions for states I and II, $f_{s,e}^{I,II}$ and $f_{s,i}^{I,II}$, in association with these load transfer models.

3.1 Load transfer for the pile tip

Without loss of generality, the relationship between the stress under the pile tip or unit ultimate end-bearing $q_b(z)$ and the effective vertical stress $\sigma'_v(z)$ can be estimated by [11]

$$q_b(z) = N_q \sigma'_v(z) \quad (21)$$

where N_q is a bearing capacity factor which mainly depends on the soil description [11]. Depending on the plugged states, the corresponding tip resistance can be calculated as

$$Q_b(z) = A_{tip} q_b(z) = \begin{cases} \pi(r_e^2 - r_i^2) q_b(z), & \text{(I) \& (II)} \\ \pi r_e^2 q_b(z), & \text{(III)} \end{cases} \quad (22)$$

The relation between $Q_b(L)$ and u_b can be approximated by [27], [28]

$$u_b = \frac{\eta(1 - \nu_b) Q_b(L)}{4r_e G_b} \quad (23)$$

where η is the effective parameters of pile tip displacement, $\eta \in [0.5, 1]$, ν_b and G_b are Poisson's ratio and shear modulus of the soil below the pile tip.

Thus Eqs. (21)-(23) can be used for the boundary condition (12) of the basic equation of load transfer (9) as well as the displacement and axial force responses given by Eqs. (13) and (15). Furthermore, for a specific purpose, the limiting conditions derived from other load-settlement relationships would be also used as an alternative to avoid unrealistic estimations.

3.2 Load transfer for external pile-soil interaction

As expressed by Eqs. (3), (4), external unit skin friction and unit stiffness coefficient can be determined for state III. For states I and II, we may derive from an equivalent form as following [10], [18], [29]

$$f_{s,e}^{I,II} = K_e \sigma'_{v,e} \tan \delta_e \quad (24)$$

where δ_e is the pile-soil friction angle at the external interface, K_e is the lateral earth pressure coefficient which can be estimated by [29]

$$K_e = K_{0,e} n_{K,e}$$

$$K_{0,e} = 1 - \sin \varphi_e \quad (25)$$

In (25), φ_e is the angle of shearing resistance of surrounding soil, $n_{K,e}$ is in situ coefficient that is summarized and classified in [30]. Effective vertical soil stress $\sigma'_{v,e}$ can be calculated by the following equation

$$\sigma'_{v,e} = \gamma_e z \quad (26)$$

where γ_e is the effective unit weight of the external surrounding soil.



3.3 Load transfer for internal pile-soil interaction

Due to the arching effect during pile driving, parameters of the internal soil will be changed accordingly, from elastic model to rigid model [1]-[4], [18], and internal unit skin friction tends to zero as state III occurs. Therefore, we consider here an equivalent internal unit skin friction for states I and II proposed by De Nicola and Randolph [3], like as the form of $f_{s,i}^{I,II}$

$$f_{s,i}^{I,II} = K_i \sigma'_{v,i} \tan \delta_i \quad (27)$$

where $K_i, \sigma'_{v,i}, \delta_i$ have the same definitions as $K_e, \sigma'_{v,e}, \delta_e$ but for the internal pile-soil interaction. The profiles of K_i are illustrated in Fig. 1.d, and an equilibrium of a soil segment involved $\sigma'_{v,i}$ is shown in Fig. 1.c. In these diagrams, h denotes the variable length of soil plug from the pile tip, h_1 and h_2 are respectively length of upper and lower soil columns, $h_2 = 10D_i$ following Fig. 1.d with D_i is the pile internal diameter. The expressions of K_i and $\sigma'_{v,i}$ relative to h are determined as below.

3.3.1 For the upper soil column, $h_2 \leq h \leq h_{plug} = h_1 + h_2$

The upper soil column act as a surcharge pressure on the lower one [3], thus the value of $\sigma'_{v,i}$ at level h is

$$\sigma'_{v,i} = \gamma_1 (h_{plug} - h) \quad (28)$$

where γ_1 is the effective soil unit weight of the upper column. K_i can be estimated by

$$\begin{aligned} K_i &= K_{0,i} n_{K,i} \\ K_{0,i} &= 1 - \sin \varphi_i \end{aligned} \quad (29)$$

with corresponding parameters $\varphi_i, n_{K,i}$ available in [29], [30].

3.3.2 For the lower soil column, $0 \leq h \leq h_2$

As shown in Fig. 1.d, the distribution of K_i in the lower soil column consists of three intervals, which can be estimated by a piecewise linear function of soil plug length h [3]

$$K_i = \begin{cases} K_{i\max}, & 0 \leq h \leq D_i \\ K_{i\max} - (K_{i\max} - K_{i\min}) \frac{h - D_i}{4D_i}, & D_i < h \leq 5D_i \\ K_{i\min}, & 5D_i < h \leq h_2 = 10D_i \end{cases} \quad (30)$$

where $K_{i\max}, K_{i\min}$ are empirical values which can be chosen as [18]

$$\begin{aligned} K_{i\max} &= 1.3 e^{-1.45PLR} \\ K_{i\min} &= 0.3 \end{aligned} \quad (31)$$

with PLR is the plug length ratio. Here, an approximation of PLR provided in [8] is used

$$PLR = (D_i / 1.4)^{0.19} \quad (32)$$

Based on the equilibrium of a soil plug segment in Fig. 1.c, the relation between $f_{s,i}^{I,II}$ and $\sigma'_{v,i}$ is described by the following differential equation [3]

$$\frac{d\sigma'_{v,i}}{dh} = -\gamma_2 - \frac{4}{D_i} f_{s,i}^{I,II} \quad (33)$$

where the effective unit weight of soil now is γ_2 , which differs γ_1 due to the soil compaction under arching effect. From Eq. (3), we would find $\sigma'_{v,i}$ using $f_{s,i}^{I,II}$ given by Eq. (27) and relative value of K_i from Eq. (30) within each interval of h as following.

3.3.2.1 Within the interval $0 \leq h \leq D_i$

In this interval, $K_i = K_{i\max}$, and the value of $\sigma'_{v,i}$ at $h = 0$ is considered to be equal to the tip resistance $q_b(z)$ given by Eq. (21) at $z = z_{fully}$, where z_{fully} is the depth at which the state III occurs. This is

$$\sigma'_{v,i}(h = 0) = q_b(z_{fully}) \quad (34)$$

With boundary condition Eq. (34), solving Eq. (33) yields the solution

$$\sigma'_{v,i} = \left(q_b(z_{fully}) + \frac{\gamma_2}{\alpha_1} \right) e^{\alpha_1 h} - \frac{\gamma_2}{\alpha_1} \quad (35)$$

where

$$\alpha_1 = 4K_{i\max} \tan \delta_i / D_i \quad (36)$$



3.3.2.2 Within the interval $5D_i < h \leq h_2 = 10D_i$

In this interval, $K_i = K_{i\min}$, and the value of $\sigma'_{v,i}$ at $h = h_2$ is considered to equal the surcharge pressure caused by the upper soil column

$$\sigma'_{v,i}(h = h_2) = \gamma_1 h_1 \quad (37)$$

with boundary condition Eq. (37), solving Eq. (33) yields the solution

$$\sigma'_{v,i} = e^{\alpha_2 h_2} \left(\gamma_1 h_1 + \frac{\gamma_2}{\alpha_2} \right) e^{\alpha_2 h} - \frac{\gamma_2}{\alpha_2} \quad (38)$$

where

$$\alpha_2 = 4K_{i\min} \tan \delta_i / D_i \quad (39)$$

3.3.2.3 Within the interval $D_i \leq h \leq 5D_i$

It is noted that the obtained expressions of $\sigma'_{v,i}$ in (35) and (38) are two particular solutions of the governing differential equation (33) at $h = D_i$ and $h = 5D_i$. Assuming that there is no stress jump at those levels of soil plug length, then the general solution of $\sigma'_{v,i}$ for this interval can be determined by

$$\sigma'_{v,i} = B_1 \left[\left(q_b + \frac{\gamma_2}{\alpha_1} \right) e^{\alpha_1 h} - \frac{\gamma_2}{\alpha_1} \right] + B_2 \left[e^{\alpha_2 h_2} \left(\gamma_1 h_1 + \frac{\gamma_2}{\alpha_2} \right) e^{\alpha_2 h} - \frac{\gamma_2}{\alpha_2} \right] \quad (40)$$

where B_1, B_2 are constants. Using Eq. (35) with $h = D_i$ and Eq. (38) with $h = 5D_i$ as two boundary conditions to (40)

$$\sigma'_{v,i}(h = D_i) = \left(q_b + \frac{\gamma_2}{\alpha_1} \right) e^{\alpha_1 D_i} - \frac{\gamma_2}{\alpha_1} \quad (41)$$

$$\sigma'_{v,i}(h = 5D_i) = e^{\alpha_2 h_2} \left(\gamma_1 h_1 + \frac{\gamma_2}{\alpha_2} \right) e^{\alpha_2 5D_i} - \frac{\gamma_2}{\alpha_2} \quad (42)$$

This will give

$$B_1 = \frac{\frac{e^{\alpha_2 h_2} \left(\gamma_1 h_1 + \frac{\gamma_2}{\alpha_2} \right) e^{\alpha_2 D_i} + \frac{\gamma_2}{\alpha_2}}{-\left(q_b + \frac{\gamma_2}{\alpha_1} \right) e^{\alpha_1 D_i} + \frac{\gamma_2}{\alpha_1}}}{\frac{\left(q_b + \frac{\gamma_2}{\alpha_1} \right) e^{\alpha_1 5D_i} - \frac{\gamma_2}{\alpha_1}}{-\left(q_b + \frac{\gamma_2}{\alpha_1} \right) e^{\alpha_1 D_i} + \frac{\gamma_2}{\alpha_1}} - \frac{e^{\alpha_2 h_2} \left(\gamma_1 h_1 + \frac{\gamma_2}{\alpha_2} \right) e^{\alpha_2 5D_i} - \frac{\gamma_2}{\alpha_2}}{-\left(q_b + \frac{\gamma_2}{\alpha_1} \right) e^{\alpha_1 D_i} + \frac{\gamma_2}{\alpha_1}}} + 1 \quad (43)$$

$$B_2 = \frac{\frac{\left(q_b + \frac{\gamma_2}{\alpha_1} \right) e^{\alpha_1 5D_i} - \frac{\gamma_2}{\alpha_1}}{-e^{\alpha_2 h_2} \left(\gamma_1 h_1 + \frac{\gamma_2}{\alpha_2} \right) e^{\alpha_2 5D_i} + \frac{\gamma_2}{\alpha_2}} + 1}{\frac{e^{\alpha_2 h_2} \left(\gamma_1 h_1 + \frac{\gamma_2}{\alpha_2} \right) e^{\alpha_2 D_i} - \frac{\gamma_2}{\alpha_2}}{-e^{\alpha_2 h_2} \left(\gamma_1 h_1 + \frac{\gamma_2}{\alpha_2} \right) e^{\alpha_2 5D_i} + \frac{\gamma_2}{\alpha_2}} - \frac{\left(q_b + \frac{\gamma_2}{\alpha_1} \right) e^{\alpha_1 5D_i} - \frac{\gamma_2}{\alpha_1}}{-\left(q_b + \frac{\gamma_2}{\alpha_1} \right) e^{\alpha_1 D_i} + \frac{\gamma_2}{\alpha_1}}} + 1 \quad (44)$$

It is noted that by using two particular solutions, the obtained result of $\sigma'_{v,i}$ in Eq. (40) is a new analytical expression, while $\sigma'_{v,i}$ was proposed to numerically solve for the interval $D_i \leq h \leq 5D_i$ in [3] and [18]. After entirely determining K_i given by Eqs. (29), (30), and $\sigma'_{v,i}$ given by Eqs. (28), (35), (38), (40), substituting their values to Eq. (44) yields four formulations of $f_{s,i}^{I,II}$ relative to the upper and lower soil columns.

3.4 Explicit formulations of the weighting coefficient

Because the internal pile-soil interaction includes four formulations of $f_{s,i}^{I,II}$ derived from various values of K_i and $\sigma'_{v,i}$ as functions of h , there are four relative formulations of the weighting coefficient p as a consequence. Clearly, the fifth formulation of p is $p=1$ as $f_{s,i}^{III}=0$ corresponding with state III. Hence it is necessary to change h to z for calculating the average value of external and internal unit skin friction in Eqs. (19)-(20). The fact is that several design criteria recommend a relation between pile outer diameter D_e and the full penetration depth z_{fully} , at which state III occurs, such as [12]



$$z_{\text{fully}} = 15D_e, \text{ for sand or gravel} \quad (45)$$

Accordingly, we can make a change of variables by using the relation (45), namely $z = z_{\text{fully}} - h$ for $z \leq 15D_e$. The obtained values of $\langle f_{s,e}^{I,II} \rangle$, $\langle f_{s,i}^{I,II} \rangle$ and the weighting coefficient p are, respectively:

- For $z \in [z_0 = 0, z_1 = z_{\text{fully}} - 10D_i]$

$$\langle f_{s,e}^{I,II} \rangle_1 = \frac{(z_1^2 - z_0^2) \gamma_e K_e \tan \delta_e}{2(z_1 - z_0)} \quad (46)$$

$$\langle f_{s,i}^{I,II} \rangle_1 = \frac{(z_1^2 - z_0^2) \gamma_i K_i \tan \delta_i}{2(z_1 - z_0)} \quad (47)$$

$$p_1 = \frac{\gamma_e K_e \tan \delta_e}{\gamma_e K_e \tan \delta_e + \gamma_i K_i \tan \delta_i} \quad (48)$$

- For $z \in [z_1 = z_{\text{fully}} - 10D_i, z_2 = z_{\text{fully}} - 5D_i]$

$$\langle f_{s,e}^{I,II} \rangle_2 = \frac{(z_2^2 - z_1^2) \gamma_e K_e \tan \delta_e}{2(z_2 - z_1)} \quad (49)$$

$$\langle f_{s,i}^{I,II} \rangle_2 = \left[\left(\gamma_1 h_1 + \frac{\gamma_2}{\alpha_2} \right) e^{\alpha_2 h_2} e^{-\alpha_2 z_{\text{fully}}} (e^{\alpha_2 z_2} - e^{\alpha_2 z_1}) - \gamma_2 (z_2 - z_1) \right] \frac{K_{i\min} \tan \delta_i}{(z_2 - z_1) \alpha_2} \quad (50)$$

$$p_2 = \frac{[(z_2^2 - z_1^2) / 2] \gamma_e K_e \tan \delta_e}{[(z_2^2 - z_1^2) / 2] \gamma_e K_e \tan \delta_e + \left[\left(\gamma_1 h_1 + \frac{\gamma_2}{\alpha_2} \right) e^{\alpha_2 h_2} e^{-\alpha_2 z_{\text{fully}}} (e^{\alpha_2 z_2} - e^{\alpha_2 z_1}) - \gamma_2 (z_2 - z_1) \right] \frac{K_{i\min} \tan \delta_i}{\alpha_2}} \quad (51)$$

- For $z \in [z_2 = z_{\text{fully}} - 5D_i, z_3 = z_{\text{fully}} - D_i]$

$$\langle f_{s,e}^{I,II} \rangle_3 = \frac{(z_3^2 - z_2^2) \gamma_e K_e \tan \delta_e}{2(z_3 - z_2)} \quad (52)$$

$$\begin{aligned} \langle f_{s,i}^{I,II} \rangle_3 = & \frac{\tan \delta_i}{z_3 - z_2} \left\{ \frac{\gamma_2}{\alpha_1} \left[K_{i\max} + \frac{(K_{i\max} - K_{i\min})(D_i - z_{\text{fully}})}{4D_i} \right] (z_2 - z_3)(B_1 + B_2) + \frac{B_1 \gamma_2 (K_{i\max} - K_{i\min})}{8D_i \alpha_1} (z_2^2 - z_3^2)(B_1 + B_2) \right. \\ & + \frac{B_1}{4D_i \alpha_1^2} \left[\frac{\gamma_2}{\alpha_1} + q_b \right] \left[e^{\alpha_1(z_2 - z_{\text{fully}})} (\alpha_1 z_2 - 1) - e^{\alpha_1(z_3 - z_{\text{fully}})} (\alpha_1 z_3 - 1) \right] (K_{i\min} - K_{i\max}) \\ & + \frac{B_2 e^{\alpha_2 h_2}}{4D_i \alpha_2^2} \left[\gamma_1 h_1 + \frac{\gamma_2}{\alpha_2} \right] \left[e^{\alpha_2(z_2 - z_{\text{fully}})} (\alpha_2 z_2 - 1) - e^{\alpha_2(z_3 - z_{\text{fully}})} (\alpha_2 z_3 - 1) \right] (K_{i\min} - K_{i\max}) \\ & + \frac{B_1 e^{-\alpha_1 z_{\text{fully}}}}{4\alpha_1^2} \left[\frac{z_{\text{fully}}}{D_i} (K_{i\min} - K_{i\max}) + (K_{i\min} - 5K_{i\max}) \right] (e^{\alpha_1 z_2} - e^{\alpha_1 z_3}) (\gamma_2 + q_b) \\ & \left. + \frac{B_2 e^{\alpha_2 h_2} e^{-\alpha_2 z_{\text{fully}}}}{4\alpha_2^2} \left[\frac{z_{\text{fully}}}{D_i} (K_{i\max} - K_{i\min}) + (K_{i\min} - 5K_{i\max}) \right] (e^{\alpha_2 z_2} - e^{\alpha_2 z_3}) (\gamma_2 + \gamma_1 h_1) \right\} \end{aligned} \quad (53)$$

$$p_3 = \frac{[(z_3^2 - z_2^2) / 2] \gamma_e K_e \tan \delta_e}{[(z_3^2 - z_2^2) / 2] \gamma_e K_e \tan \delta_e + (z_3 - z_2) \langle f_{s,i}^{I,II} \rangle_3} \quad (54)$$

where B_1, B_2 are given by Eqs. (43), (44).

- For $z \in [z_3 = z_{\text{fully}} - D_i, z_4 = z_{\text{fully}}]$

$$\langle f_{s,e}^{I,II} \rangle_4 = \frac{(z_4^2 - z_3^2) \gamma_e K_e \tan \delta_e}{2(z_4 - z_3)} \quad (55)$$

$$\langle f_{s,i}^{I,II} \rangle_4 = \left[\left(q_b z_{\text{fully}} + \frac{\gamma_2}{\alpha_1} \right) e^{-\alpha_1 z_{\text{fully}}} (e^{\alpha_1 z_4} - e^{\alpha_1 z_3}) - \gamma_2 (z_4 - z_3) \right] \frac{K_{i\max} \tan \delta_i}{(z_4 - z_3) \alpha_1} \quad (56)$$



$$p_4 = \frac{[(z_4^2 - z_3^2) / 2] \gamma_e K_e \tan \delta_e}{[(z_4^2 - z_3^2) / 2] \gamma_e K_e \tan \delta_e + \left[\left(q_b z_{\text{fully}} + \frac{\gamma_2}{\alpha_1} \right) e^{-\alpha_1 z_{\text{fully}}} (e^{\alpha_1 z_4} - e^{\alpha_1 z_3}) - \gamma_2 (z_4 - z_3) \right] \frac{K_{\text{imax}} \tan \delta_i}{\alpha_1}} \quad (57)$$

- For $z > z_{\text{fully}}$, $p_5 = 1$.

It is noted that the value of p is different in the above intervals due to the various values of skin frictions. Hence the calculated value of p at the intersection of two adjacent intervals is proposed to be the average of the two corresponding values of p in those two intervals, as represented by

$$p_{1-2} = \frac{p_1 + p_2}{2} = \frac{1}{2} \left[\frac{\gamma_e K_e \tan \delta_e}{\gamma_e K_e \tan \delta_e + \gamma_1 K_i \tan \delta_i} + \frac{[(z_2^2 - z_1^2) / 2] \gamma_e K_e \tan \delta_e}{[(z_2^2 - z_1^2) / 2] \gamma_e K_e \tan \delta_e + \left[\left(\gamma_1 h_1 + \frac{\gamma_2}{\alpha_2} \right) e^{\alpha_2 h_2} e^{-\alpha_2 z_{\text{fully}}} (e^{\alpha_2 z_2} - e^{\alpha_2 z_1}) - \gamma_2 (z_2 - z_1) \right] \frac{K_{\text{imin}} \tan \delta_i}{\alpha_2}} \right] \quad (58)$$

- For $z = z_{\text{fully}} - 5D_i$

$$p_{2-3} = \frac{p_2 + p_3}{2} = \frac{1}{2} \left[\frac{[(z_2^2 - z_1^2) / 2] \gamma_e K_e \tan \delta_e}{[(z_2^2 - z_1^2) / 2] \gamma_e K_e \tan \delta_e + \left[\left(\gamma_1 h_1 + \frac{\gamma_2}{\alpha_2} \right) e^{\alpha_2 h_2} e^{-\alpha_2 z_{\text{fully}}} (e^{\alpha_2 z_2} - e^{\alpha_2 z_1}) - \gamma_2 (z_2 - z_1) \right] \frac{K_{\text{imin}} \tan \delta_i}{\alpha_2}} + \frac{[(z_3^2 - z_2^2) / 2] \gamma_e K_e \tan \delta_e}{-[(z_3^2 - z_2^2) / 2] \gamma_e K_e \tan \delta_e + (z_3 - z_2) \langle f_{s,i}^{I,II} \rangle_3} \right] \quad (59)$$

- For $z = z_{\text{fully}} - D_i$

$$p_{3-4} = \frac{p_3 + p_4}{2} = \frac{1}{2} \left[\frac{[(z_3^2 - z_2^2) / 2] \gamma_e K_e \tan \delta_e}{[(z_3^2 - z_2^2) / 2] \gamma_e K_e \tan \delta_e + (z_3 - z_2) \langle f_{s,i}^{I,II} \rangle_3} + \frac{[(z_4^2 - z_3^2) / 2] \gamma_e K_e \tan \delta_e}{[(z_4^2 - z_3^2) / 2] \gamma_e K_e \tan \delta_e + \left[\left(q_b z_{\text{fully}} + \frac{\gamma_2}{\alpha_1} \right) e^{-\alpha_1 z_{\text{fully}}} (e^{\alpha_1 z_4} - e^{\alpha_1 z_3}) - \gamma_2 (z_4 - z_3) \right] \frac{K_{\text{imax}} \tan \delta_i}{\alpha_1}} \right] \quad (60)$$

- For $z = z_{\text{fully}}$

$$p_{4-5} = \frac{p_4 + p_5}{2} = \frac{1}{2} \left[\frac{[(z_4^2 - z_3^2) / 2] \gamma_e K_e \tan \delta_e}{[(z_4^2 - z_3^2) / 2] \gamma_e K_e \tan \delta_e + \left[\left(q_b z_{\text{fully}} + \frac{\gamma_2}{\alpha_1} \right) e^{-\alpha_1 z_{\text{fully}}} (e^{\alpha_1 z_4} - e^{\alpha_1 z_3}) - \gamma_2 (z_4 - z_3) \right] \frac{K_{\text{imax}} \tan \delta_i}{\alpha_1}} + 1 \right] \quad (61)$$

Next, substituting obtained values of weighting coefficient p , and k_e^{III} given by Eq. (4) into Eq. (10), to give the displacement and axial force responses given by Eqs. (13)-(15).

4. Numerical examination

In this example, we will apply the equivalent stiffness-based load transfer model to analyze a jacked open-ended pile. Surrounding soil is considered to be homogeneous, and there is no bearing stratum at the pile end. The fully plugged state is considered to occur when $z_{\text{fully}} = 15D_e \simeq 15D_i$. The input parameters of the pile, soil are given as follow:

Pile: $L = 2m, D_e = 141mm, D_i = 131mm, z_{\text{fully}} = 15D_i, E_p = 210GPa, \rho_p = 7850kg/m^3$

Soil: $\gamma_s = 18 kN/m^3, E_s = 10MPa, v_s = 0.3, \varphi = 30^\circ, G_s = \frac{E_s}{2(1+v_s)} \left[1 - \frac{2v_s^2}{1-v_s} \right]$.

To calculate the vertical effective stress $\sigma'_{v,i}$ of soil plug, Eqs. (28), (35), (38) and (40) are used corresponding with four profiles of K_i within four intervals of the soil columns (see Fig. 1.d). The input parameters are the pile diameters, effective unit weights of the soil, and K_i . Fig. 2 represents the distribution of the ratio $\sigma'_{v,i} / q_b(L)$ versus the ratio h / D_i with the length of the upper soil column h_1 varies. As indicated in Eqs. (35), (38) and (40), vertical effective stress $\sigma'_{v,i}$ in the lower soil column are exponentially distributed to plug length h , while the one given by Eq. (28) in the upper soil column decreases linearly with h . In the upper soil column, within $h / D_i = [10, 15]$, the curve denoted by the blue line (only visible as zooming in) shows that $\sigma'_{v,i}$



decreases linearly with h , which acts as surcharge pressure on the lower soil column. In the lower soil column, within $h/D_i = [0, 10]$, the curve (black line) decreases from the unit tip resistance $q_b(L)$ to a smaller one at $h/D_i = 1$, then peaks near $h/D_i = 2$ very fast, after that reduces quickly to a value almost equal or greater than q_b at $h/D_i = 4$ (red line), and reduces more slowly to a minimum value at the interface of the two columns, $h/D_i = 10$ (magenta line). It is seen that surcharge pressure caused by the upper soil column has a great effect on $\sigma'_{v,i}$ in the lower one, i.e. the higher the value of h_1 , the larger the peak value of $\sigma'_{v,i}$ will be. As observed in two internal diameters D_i from the pile tip, the maximal value of $\sigma'_{v,i}$ is near $h/D_i = 2$. The slope of the curve $\sigma'_{v,i}$ within $h/D_i = [2; 10]$ shows the arching formation (according to Paikowsky [31]). High rising of $\sigma'_{v,i}$ provides a suitable interpretation of the arching mechanism and gives soil plug capacity. The position of the peak value of $\sigma'_{v,i}$ coincides with the empirical result of Lüking and Kempfert [32], who found that the arching exists only at the last two pile diameters. Clearly, the distribution of $f_{s,i}$ the soil plug is similar to that of $\sigma'_{v,i}$, from which it is demonstrated that the shear resistance is concentrated over $1D_i \div 2D_i$ above the pile base as remarks from tests by De Nicola and Randolph [3], Lehane and Gavin [8].

The purpose of Fig. 3 is to compare the differences of axial force $P(z)$ in three states of the driving process: unplugged (state I), partially plugged (state II) and fully plugged (state III). As shown in this Fig, the slope of the curve is greatest for state III and decreases gradually for the others, state II and I, respectively. Because the soil resistance to the pile increases with the penetration depth of the pile into the soil, so the value of $P(z)$ is minimum in state I, and increases gradually to state III. For each state, there is a clear difference in the correlation of $P(z)$ between the two types of piles CEP and OEP. It can be seen that, in unplugged and partially plugged states, when the penetration depth of pile in the soil is small $z_{penetrated} < 10D_i$, the soil resistance acting on the OEP is much less than that of CEP, so the curve $P(z)$ of the two types of piles has large spacing. Whereas in the fully plugged state, when $z_{penetrated} > 10D_i$, initially the two curves corresponding to the two types of piles are placed far apart, after that, gradually as z increases, the soil resistance is nearly equal, making the OEP tend to resemble CEP, resulting in the two curves being nearly identical.

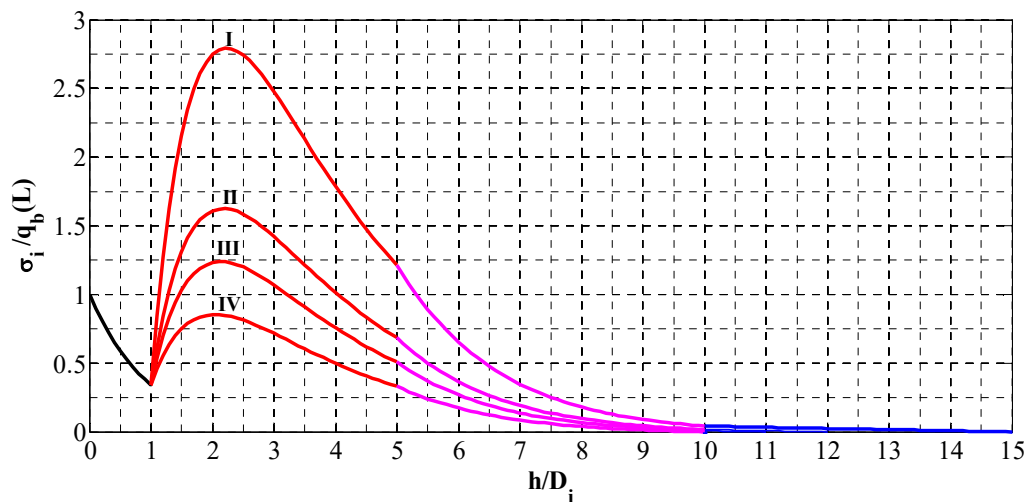


Fig. 2. σ'_i / q_b versus h/D_i with h_1 varies I: $h_1/D_i = 5$; II: $h_1/D_i = 2$; III: $h_1/D_i = 1$; IV: $h_1/D_i = 0$

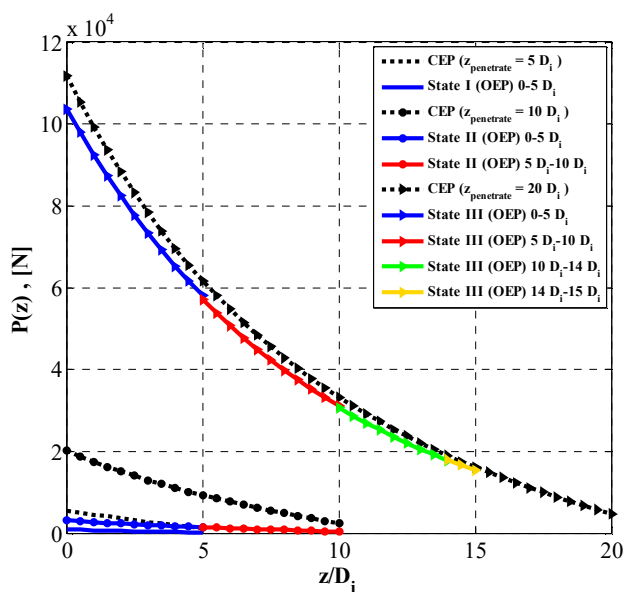


Fig. 3. $P(z)$ versus z/D_i in the unplugged, partially plugged, and fully plugged states

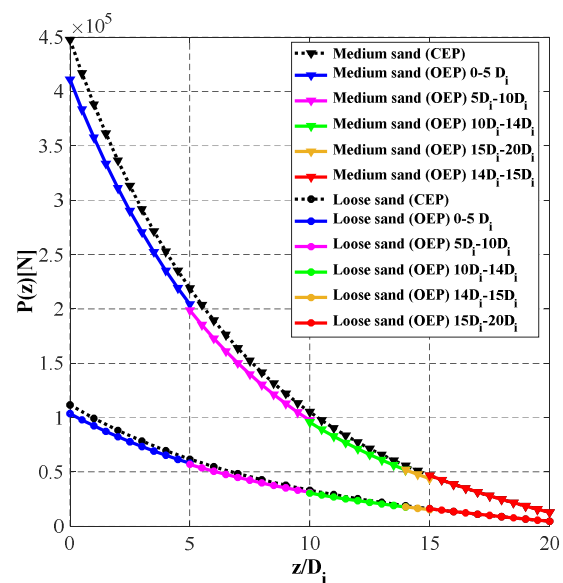


Fig. 4. $P(z)$ versus z/D_i for medium and loose sandy soil

OEP: open-ended pile; CEP: close-ended pile



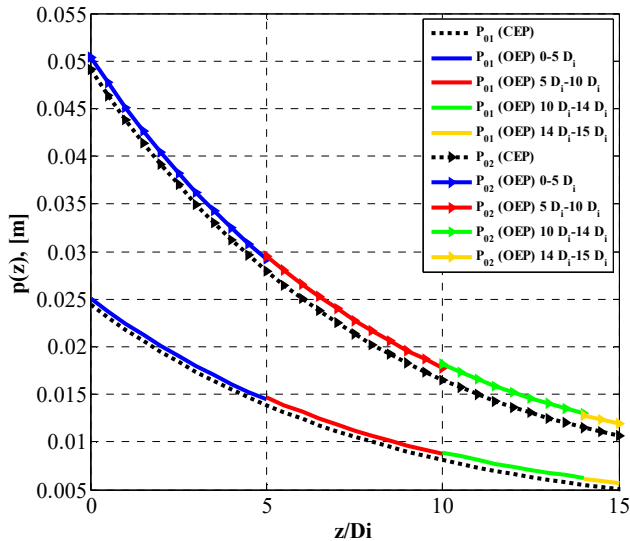
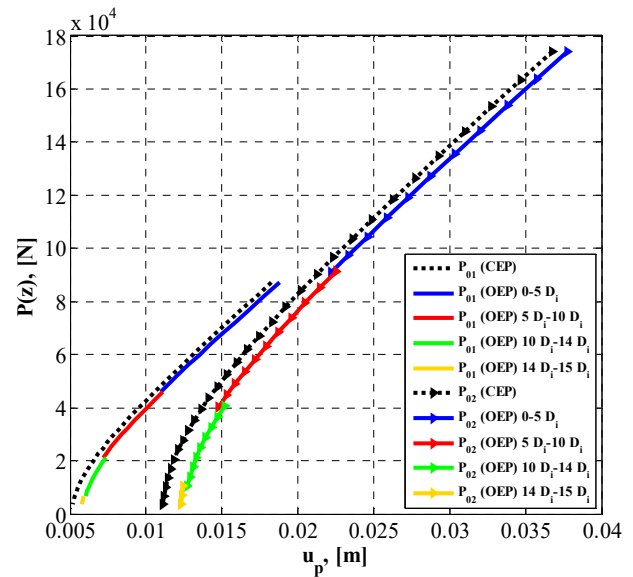
Fig. 5. u_p versus z/D_i with P_0 variesFig. 6. $P(z)$ versus u_p with P_0 varies

Fig. 4 indicates the variation of the axial force $P(z)$ according to the depth z corresponding to different types of soil, respectively medium and loose sandy soil. With the exponential decrease, the slope of medium sand's curve is greater than loose sand's. Considering the value of $P(z)$, the soil density of medium sand is higher, thus the force required to drive piles to the ground is higher than others. Besides, for both types of soil, when comparing CEP and OEP, the value of $P(z)$ will be much different at the started piling states, with $z/D_i = [0;5]$, $z/D_i = [5;10]$, or $z/D_i = [10;14]$, but with $z/D_i = [14;15]$, the OEP tends to the fully plugged state which is similar to the CEP, hence the curve $P(z)$ of the two types of piles are the same.

The variation of the axial displacement u_p according to the penetration depth of the pile z under the driving force at the pile head P_0 is shown in Fig. 5. Consider the process of piling, from $z/D_i = [0;5]$ to $z/D_i = [14;15]$, when increasing the pressure from $P_{01} = 25P_b$ to $P_{02} = 50P_b$, the curve shape changes slightly, but the slope of the curve increases. With the pressure $P_0 = P_{01}$, the axial displacement of the OEP decreased exponentially, specifically the displacement at the pile tip (0.025 m) was 6.6 times greater than the displacement at the pile head (0.0038 m), corresponding to $z/D_i = [0;5]$. Similarly, the largest displacements at intervals $z/D_i = [5;10]$, $z/D_i = [10;14]$ and $z/D_i = [14;15]$ are 0.014 m, 0.0089 m and 0.0061 m, respectively. When compared with CEP, it can be seen that the displacement of OEP is always larger than that of CEP, and the largest value is at $z/D_i = [14;15]$. Furthermore, as the pressure increases, the difference in displacement between OEP and CEP increases, due to the frictional state of the soil plug. For example, at $z = 10D_i$, the difference value when $P_0 = P_{01}$ is 0.00086 m, while with $P_0 = P_{02}$, this value is 0.00171 m.

Fig. 6 shows the relationship between the axial force $P(z)$ and the pile displacement u_p under different driving forces at the pile head P_0 . As we can see, when $z/D_i = [0;5]$, $z/D_i = [5;10]$ or $z/D_i = [10;14]$, the bearing capacity at the pile head was not stimulated, and only properties of the pure friction pile are shown. As P_0 increased from $P_{01} = 25P_b$ to $P_{02} = 50P_b$, the working load at the pile head developed gradually, the distribution of axial force was roughly linear and then transformed into a curve when $z/D_i = [14;15]$, whose slopes got steeper as the depth became deeper. The slope in the vicinity of the pile end changed evidently. The larger the load, the more obvious the change in slope appeared. This meant that the axial force decreased sharply, largely due to the contribution of soil plug skin friction. With the pressure $P_0 = P_{01}$, when u_p increases, the axial force of OEP increases, specifically the axial force at the pile tip in the ranges $z/D_i = [0;5]$, $z/D_i = [5;10]$, $z/D_i = [10;14]$ and $z/D_i = [14;15]$ are 0.674×10^4 , 2.125×10^4 , 4.609×10^4 , and 8.714×10^4 N, respectively. When compared with CEP, it can be seen that with the same displacement u_p , the axial force of OEP is always smaller than that of CEP, and the difference in axial force value between these two types of piles seems to increase when P_0 increases. For instance, at $u_p = 0.012$ m, with $P_0 = P_{01}$, the difference force value between OEP and CEP is 0.334×10^4 N, while for $P_0 = P_{02}$ this value is 2.111×10^4 N. It can be concluded that the larger the pile driving forces, the clearer the difference in displacement response of the two types of piles OEP and CEP.

5. Conclusions

The main intent of the paper is to develop an equivalent stiffness-based load transfer model of an axially loaded open-ended pipe pile. Based on the findings of this study, the following conclusions can be drawn:

- First, a load transfer model of an axially loaded open-ended pile is established in which the external and internal skin frictions, as well as the pile tip resistance, are taken into account. Based on the dual approach, the replacement of the sum of unit stiffnesses in the basic differential equation of load transfer by a weighted average of equivalent unit stiffnesses is made, in which equivalent unit stiffnesses are derived from the unit stiffness determined from the elastic theory in the fully plugged state. A normalized dimensionless weighting coefficient p is introduced in considering the contributions of external and internal unit skin frictions to the total unit skin frictions in the form of average value with the penetration depth. Analysis of weighting coefficients related to the boundary limit of plugged states shows $p = 1/2$ when transitioning from unplugged state to partially plugged state, and $p = 1$ when transitioning from partially plugged state to fully plugged state. The analytical expressions of displacement and axial force responses then can be determined.



- b) Next, the equivalent stiffness-based load transfer model is applied to a jacked open-ended pile concerning semi-empirical models of external and internal unit skin frictions in which the internal lateral earth pressure coefficient is a piecewise linear function of soil plug length. The result leads to explicit expressions of weighting coefficient p corresponding with those semi-empirical models.
- c) The examination of a jacked open-ended pile shows that there is a good agreement between numerical results with empirical ones available in the literature about the behavior of internal effective stress. Next, qualitative comparisons between the open-ended pile with a close-ended pile provide detailed descriptions of the plugging effect on the displacement and axial force responses, as well as different requirements for the driving force in various penetration depths and soil conditions.
- d) It appears that this equivalent stiffness-based load transfer model has a large potential in exploring wider classes of open-ended pile driving.

Author Contributions

N.N. Linh planned the scheme, initiated the project, and suggested the mathematical model; N.A. Ngoc solved the proposed mathematical model; N.V. Kuu examined the theory validation; N.D. Diem checked the formulation and the obtained results. The manuscript was written through the contribution of all authors. All authors discussed the results, reviewed, and approved the final version of the manuscript.

Conflict of Interest

The authors declared no potential conflicts of interest with respect to the research, authorship, and publication of this article.

Nomenclature

Latin symbols

A_e, A_i	Outer and inner surface areas of the pile [m^2]
A_p	Section area of the pile [m^2]
D_e, D_i	Outer and inner diameters of the pile [m]
E_p	Elastic modulus of the pile [N/m^2]
E_s	Elastic modulus of the soil [N/m^2]
f_{se}, f_{si}	External and internal unit skin friction [N/m^2]
G_b	Shear modulus of the base soil [N/m^2]
h	Variable length of soil plug from the pile tip [m]
h_1, h_2	Length of upper and lower soil columns [m]
h_{plug}	Total length of soil plug [m]
K	Lateral earth pressure coefficient
k_e, k_i	External and internal unit stiffness coefficients [N/m^3]
L	Full penetration length [m]
N_q	Bearing capacity factor
p	Normalized dimensionless weighting coefficient
P	Axial force of the pile [N]
PLR	The plug length ratio
Q_b	Tip resistance [N/m^2]
r_e, r_i	Outer and inner radius of the pile [m]
u_b	Base settlement [m]
u_p	Axial displacement of the pile [m]
ν_b	Poisson's ratio of the base soil
z	Penetration depth from the ground surface [m]

Greek symbols

δ_e, δ_i	External and internal pile-soil friction angle [rad]
γ_1, γ_2	Effective unit weight of upper and lower soil columns
γ_e	Effective unit weight of the external soil [N/m^3]
η	Effective parameters of pile tip displacement
ϕ	Angle of shearing of soil [rad]
μ	Ratio of shaft-pile stiffness [m^{-1}]
$\sigma'_{v,e}, \sigma'_{v,i}$	Effective vertical stress outside and inside [N/m^2]
ζ_e	Effective parameter of the outer pile radius
δ_e, δ_i	External and internal pile-soil friction angle [rad]
γ_1, γ_2	Effective unit weight of upper and lower soil columns [N/m^3]
γ_e	Effective unit weight of external soil [N/m^3]

Subscripts

e	External
i	Internal
s	Skin

Superscripts

I	Unplugged state
II	Partially plugged state
III	Fully plugged state

References


- [1] Paik, K. H., & Lee, S. R, Behavior of soil plugs in open-ended model piles driven into sands, *Marine Georesources & Geotechnology*, 11(4), 1993, 353-373.
- [2] Paikowsky, S. G., Whitman, R. V., & Baligh, M. M, A new look at the phenomenon of offshore pile plugging, *Marine Georesources & Geotechnology*, 8(3), 1989, 213-230.
- [3] De Nicola, A., & Randolph, M. F, The plugging behaviour of driven and jacked piles in sand, *Geotechnique*, 47(4), 1997, 841-856.
- [4] Randolph, M. F., Leong, E. C., & Houlsby, G. T, One-dimensional analysis of soil plugs in pipe piles, *Geotechnique*, 41(4), 1991, 587-598.
- [5] Jeong, S., & Ko, J, Inner skin friction of open-ended piles considering the degree of soil plugging, *Japanese Geotechnical Society Special Publication*, 2(37), 2016, 1327-1332.
- [6] Liu, J. W., Zhang, Z. M., Yu, F., & Xie, Z. Z, Case history of installing instrumented jacked open-ended piles, *Journal of Geotechnical and Geoenvironmental Engineering*, 138(7), 2012, 810-820.
- [7] Al-Soudani, W. H., Albusoda, B. S, An experimental study on bearing capacity of steel open ended pipe pile with exterior wings under compression load, *Geotechnical and Geological Engineering*, 39(2), 2021, 1299-1318.
- [8] Lehane, B. M., Gavin, K. G, Base resistance of jacked pipe piles in sand, *Journal of Geotechnical and Geoenvironmental Engineering*, 127(6), 2001, 473-480.
- [9] Gudavalli, S. R., Safaqaq, O., & Seo, H, Effect of soil plugging on axial capacity of open-ended pipe piles in sands, In *Proceedings of the 18th*





International Conference on Soil Mechanics and Geotechnical Engineering, 2013, 1487-1490.


- [10] Han, F., Ganju, E., Salgado, R., Prezzi, M., Comparison of the load response of closed-ended and open-ended pipe piles driven in gravelly sand, *Acta Geotechnica*, 14(6), 2019, 1785-1803.
- [11] API (American Petroleum Institute), Geotechnical and foundation design considerations, Washington DC, USA: API, 2011.
- [12] Guo, Y., Yu, X. B., Design and analyses of open-ended pipe piles in cohesionless soils, *Frontiers of Structural and Civil Engineering*, 10(1), 2016, 22-29.
- [13] Henke, S., Grabe, J., Numerical investigation of soil plugging inside open-ended piles with respect to the installation method, *Acta Geotechnica*, 3(3), 2008, 215-223.
- [14] Henke, S., Large deformation numerical simulations regarding soil plugging behaviour inside open-ended piles, In: *ASME 2012 31st international conference on ocean, offshore and arctic engineering*, American Society of Mechanical Engineers, 2012, 37-46.
- [15] Wang, T., Zhang, Y., Bao, X., Wu, X., Mechanisms of soil plug formation of open-ended jacked pipe pile in clay, *Computers and Geotechnics*, 118, 2020, 103334.
- [16] Li, L., Wu, W., Hesham El Naggar, M., Mei, G., Liang, R., DEM analysis of the sand plug behavior during the installation process of open-ended pile, *Computers and Geotechnics*, 109, 2019, 23-33.
- [17] Li L., Wu W., Liu H., Lehane B., DEM analysis of the plugging effect of open-ended pile during the installation process, *Ocean Engineering*, 220, 2021, 108375.
- [18] Liu, J., Guo, Z., Han, B., Load transfer of offshore open-ended pipe piles considering the effect of soil plugging, *Journal of Marine Science and Engineering*, 7(9), 2019, 313.
- [19] N. D. Anh. Duality in the analysis of responses to nonlinear systems. *Vietnam Journal of Mechanics*, 32, (4), 2010, 263-266.
- [20] Anh, N. D., Hieu, N. N., Linh, N. N., A dual criterion of equivalent linearization method for nonlinear systems subjected to random excitation, *Acta Mechanica*, 223(3), 2012, 645-654.
- [21] Anh, N. D., Linh, N. N., A weighted dual criterion of the equivalent linearization method for nonlinear systems subjected to random excitation, *Acta Mechanica*, 229(3), 2018, 1297-1310.
- [22] Anh, N. D., A comprehensive review on dual approach to the vibration analysis: Some dual techniques and application, *Vietnam Journal of Mechanics*, 42(1), 2020, 1-14.
- [23] Anh, N. D., Hai, N. Q., Hieu, D. V., The equivalent linearization method with a weighted averaging for analyzing of nonlinear vibrating systems, *Latin American Journal of Solids and Structures*, 14(9), 2017, 1723-1740.
- [24] Hieu, D. V., Hai, N. Q., Analyzing of nonlinear generalized duffing oscillators using the equivalent linearization method with a weighted averaging, *Asian Research Journal of Mathematics*, 2018, 1-14.
- [25] Hieu, D. V., Hai, N. Q., Hung, D. T., The equivalent linearization method with a weighted averaging for solving undamped nonlinear oscillators, *Journal of Applied Mathematics*, 2018, 1-15.
- [26] Dang, V. H., Nguyen, D. A., Le, M. Q., Ninh, Q. H., Nonlinear vibration of microbeams based on the nonlinear elastic foundation using the equivalent linearization method with a weighted averaging, *Archive of Applied Mechanics*, 90(1), 2020, 87-106.
- [27] Randolph, M. F., & Wroth, C. P., Analysis of deformation of vertically loaded piles, *Journal of the Geotechnical Engineering Division*, 104(12), 1978, 1465-1488.
- [28] Xiao, H. B., Zhang, C. S., Wang, Y. H., & Fan, Z. H., Pile-soil interaction in expansive soil foundation: Analytical solution and numerical simulation, *International Journal of Geomechanics*, 11(3), 2011, 159-166.
- [29] Miller, G. A., & Lutenecker, A. J., Influence of pile plugging on skin friction in overconsolidated clay, *Journal of Geotechnical and Geoenvironmental Engineering*, 123(6), 1997, 525-533.
- [30] Zhang, Q. Q., Li, S. C., Liang, F. Y., Yang, M., & Zhang, Q., Simplified method for settlement prediction of single pile and pile group using a hyperbolic model, *International Journal of Civil Engineering*, 12(2), 2014, 146-159.
- [31] Paikowsky, S. G., A static evaluation of soil plug behavior with application to the pile plugging problem, Ph.D. Thesis., Massachusetts Institute of Technology, 1989.
- [32] Lüking, J., & Kempfert, H. G., Untersuchung der Pfropfenbildung an offenen Verdrängungspfählen, *Bautechnik*, 89(4), 2012, 264-274.

ORCID iD

Nguyen Ngoc Linh  <https://orcid.org/0000-0002-6724-462X>

Nguyen Anh Ngoc  <https://orcid.org/0000-0001-7322-3940>

Nguyen Van Kuu  <https://orcid.org/0000-0002-2073-9596>

Nguyen Dang Diem  <https://orcid.org/0000-0002-1295-8238>



© 2021 Shahid Chamran University of Ahvaz, Ahvaz, Iran. This article is an open access article distributed under the terms and conditions of the Creative Commons Attribution-NonCommercial 4.0 International (CC BY-NC 4.0 license) (<http://creativecommons.org/licenses/by-nc/4.0/>).

How to cite this article: Linh N.N., Ngoc N.A., Kuu N.V., Diem N.D. Weighted dual approach to an equivalent stiffness-based load transfer model for jacked open-ended pile, *J. Appl. Comput. Mech.*, 7(3), 2021, 1751-1763.
<https://doi.org/10.22055/JACM.2021.37430.3013>

Publisher's Note Shahid Chamran University of Ahvaz remains neutral with regard to jurisdictional claims in published maps and institutional affiliations.

